Journal of Photochemistry and Photobiology A: Chemistry 201 (2009) 81–86

Contents lists available at ScienceDirect

Journal of Photochemistry and Photobiology A: Chemistry

journal homepage: www.elsevier.com/locate/jphotochem

Mesoporous materials incorporating a zinc(II) complex: Synthesis and direct luminescence quantum yield determination

Daniela Aiello[a], Rosario Aiello[a], Flaviano Testa[a], Tonino Martino[b], Iolinda Aiello[b], Massimo La Deda[b], Mauro Ghedini[b,*]

[a] Department of Chemical Engineering and Materials, University of Calabria, 87036 Arcavacata di Rende (CS), Italy
[b] Centro di Eccellenza CEMIF.CAL, LASCAMM, CR-INSTM Unità della Calabria and Licryl, Department of Chemistry, University of Calabria, 87036 Arcavacata di Rende (CS), Italy

ARTICLE INFO

Article history:
Received 19 May 2008
Received in revised form
15 September 2008
Accepted 4 October 2008
Available online 15 October 2008

Keywords:
Mesoporous materials
Grafting post-synthesis
One-pot synthesis
Functionalization
Zinc(II) complexes
Schiff bases
Luminescence
Emission quantum yield

ABSTRACT

New luminescent inorganic–organic hybrid materials incorporating the luminescent zinc(II) complex ZnL_2 (λ_{em} = 457 nm and Φ_{em} = 4.4% reference values for ZnL_2; HL = chelating ligand resulting from the reaction between salicylaldehyde and 3-aminopropyltriethoxysilane), covalently bonded to different types of mesoporous silica hosts (namely MCM-41, MCM-48 and SBA-15), were prepared via both the methods of grafting post-synthesis (GPS) and one-pot synthesis (OPS). The products obtained, which form the GPS [(GPS)(Zn/MCM-41), (GPS)(Zn/MCM-48), (GPS)(Zn/SBA-15)] and the OPS [(OPS)(Zn/MCM-41), (OPS)(Zn/MCM-48), (OPS)(Zn/SBA-15)] series, contain the ZnL_2 guest covalently bonded to the silica framework through silicon–oxygen bonds formed when the silane group is placed at the periphery of the Zn(II) coordination sphere. GPS and OPS materials were characterized by powder X-ray diffraction, N_2 adsorption/desorption, thermogravimetric analysis (TGA) and UV/vis spectroscopy. For the new mesoporous materials the emission quantum yield (EQY) was measured by means of an integrating sphere combined with a spectrofluorimeter. The ZnL_2 loading (measured by the ZnL_2/SiO_2 ratio calculated from TGA data) for MCM-41 appears to be independent of the synthesis procedure, whereas, for both MCM-48 and SBA-15, the ZnL_2/SiO_2 ratio of the materials obtained via OPS is about four times higher than products obtained from GPS. The ZnL_2 loaded GPS and OPS series show λ_{em} maxima at about 485 and 455 nm, respectively. Moreover, with reference to EQY (GPS)(Zn/SBA-15) and (OPS)(Zn/SBA-15), although featuring ZnL_2/SiO_2 ratios of 0.13 and 0.45, respectively, they showed similar EQY values: 2% and 5%. On the contrary, (GPS)(Zn/MCM-41) and (OPS)(Zn/MCM-41) which give similar ZnL_2/SiO_2 ratios (0.09 and 0.14) exhibit very different EQY, i.e. 2% and 22%, respectively.

1. Introduction

The immobilization of guest species into porous inorganic solids has extensively been investigated to construct functional supramolecular materials [1]. The resulting materials can exhibit unique physicochemical properties controlled by the states of guest species as well as the nature of the porous solids.

The mesoporous silica prepared by supramolecular templating method possesses advantages such as controlled pore openings, large surfaces area and low dimensional pore geometry for the guest organization. The possible applications of this class of materials include adsorbents, catalysts and their supports, and optoelectronics materials [2,3].

In the field of optical materials, mesostructured materials fall in the range between nanoporous host such as zeolites that can align small molecules and patterned micron-scale photonic band gap materials [4]. However, the mesopore size range presents several possible advantages for optical applications. The high surface area creates the potential to dope materials at higher concentrations without self-interactions. Besides, the meso size range, 2–30 nm, is attractive for producing size-confined structures such as quantum dots [5] or nanowires [6].

Numerous studies have been performed on modification of mesoporous materials to increase their potential applicability. It was demonstrated that the direct introduction of functional molecules in the course of the one-pot synthesis of mesoporous materials and grafting post-synthesis techniques were two efficient processes.

These two techniques have been utilized to incorporate fluorescent dyes into mesoporous materials, obtaining the so-called luminescent hybrid mesoporous silica (LHMS) [7]; in fact, the

* Corresponding author. Tel.: +39 0984492062; fax: +39 0984492066.
E-mail address: m.ghedini@unical.it (M. Ghedini).

1010-6030/$ – see front matter © 2008 Elsevier B.V. All rights reserved.
doi:10.1016/j.jphotochem.2008.10.001

advantage of an inorganic matrix embedded with functional chromophores [8–13] is the more rigid environment which stabilizes the luminescent complexes and significantly increases material photostability [12,14,15].

In the last five years many research groups have studied lanthanides complexes embedded into mesoporous materials [16–23]; these studies are connected with the major subject of lanthanide-doped organic–inorganic hybrid materials, within the development of optical materials such as high efficiency and stable solid-state lasers, new fiber amplifiers and sensors, devices with upconversion, fast photochromic and non-linear responses, etc. Their interest relies on the possibility of combining properties of hybrid materials (shaping, tunable refractive index and mechanical properties, corrosion protection, specific adhesion, etc.) and the well-known luminescence of lanthanide ions [24]. LHMS include materials incorporating the well-studied Ru-bipy derived complexes [25,26], organic dyes [27,7], Schiff-base groups chelating Zn^{2+} or Cu^{2+} [13].

The photophysical characterization of LHMS on film or solid is mainly performed by means of emission spectroscopy and lifetime measurement. If LHMS embeds europium complexes, then the evaluation of the emission quantum yield (EQY) can be performed; in fact, on the basis of the corrected emission spectrum and the observed luminescence lifetime of the $^5D_0$ emitting level of Eu^{3+} ion, the EQY of the sample can be calculated according to the method described elsewhere [20,28,29]; in the cases of LHMS films or solids embedding other metals, up to now, no EQY is reported. This should be ascribed to the difficulty in determining the EQY on solid or film samples, which is a more complex procedure than the corresponding solution measurement and requires an integrating sphere and proper excitation sources. Nevertheless, the lack of this value does not allow a comparison among the photophysics of different chromophores embedded in LHMS, or between the same chromophore before and after immobilization in mesoporous materials, or the evaluation of the photophysical properties of LHMS with a fluorophore incorporated by two different methods, e.g. one-pot synthesis and grafting post-synthesis.

We are currently involved in the synthesis and characterization of photoactive materials [30], and recently we have extended our interests to light emitting species supported on inorganic mesoporous materials; here we compare two different synthesis protocols, grafting post-synthesis (GPS) and one-pot synthesis (OPS), which allow for the incorporation of the blue-emitting ZnL_2 complex (see Section 2) on different mesoporous hosts, MCM-41, MCM-48 and SBA-15 materials. MCM-41 has a one-dimensional, hexagonally ordered, unconnected but regular cylindrical pore structure ($S_{BET} \sim 1100\,m^2/g$, $D_{pore} \sim 30$ Å); MCM-48 consists of an uniform array of tubular pores which are 3D connected ($S_{BET} \sim 1500\,m^2/g$, $D_{pore} \sim 33$ Å); SBA-15 exhibits a regular two-dimensional array of tubular channels ($S_{BET} \sim 800\,m^2/g$, $D_{pore} \sim 50$ Å). Because of the differences in their pore dimension and structure, these materials are suitable hosts for investigating the effect of confinement or incorporation of organic and inorganic guest molecules [31,32]. The properties of the mesoporous solid products obtained by grafting post-synthesis [GPS series: (GPS)(Zn/MCM-41), (GPS)(Zn/MCM-48), (GPS)(Zn/SBA-15)] were compared with those directly synthesized through one-pot synthesis [OPS series: (OPS)(Zn/MCM-41), (OPS)(Zn/MCM-48), (OPS)(Zn/SBA-15)]. The emission spectra are reported and the EQY is measured by means of an integrating sphere. The topology and the photophysical properties of both series of products were examined and the differences arising from the different synthesis methods are discussed with reference to the effect of spatial pore arrangement on the host product.

2. Experimental

2.1. Materials

Tetraethyl orthosilicate 99% (TEOS), 3-aminopropyltriethoxysilane 97% (APTES), hexadecyltrimethylammonium bromide (CTABr), triblock copolymer Pluronic P123 (EO_{20}-PO_{70}-EO_{20}), salicylaldehyde 99%, zinc(II) acetate dihydrate and ethanol 99% were used as received. Ultrapure water was used throughout the work and obtained from Milli-Q equipment by Millipore.

2.2. Grafting post-synthesis method

2.2.1. Preparation of the ligand HL

Salicylaldehyde (21 mmol, 2.32 g) was added to 4.44 ml of APTES (19 mmol, 4.21 g) in ethanol (4 ml). The solution was refluxed for 5 h under constant stirring. The crude product obtained after evaporation of the solvent under reduced pressure was suspended in chloroform and filtered through a Celite column. The HL ligand obtained was a green-yellow oil which was stored at −15 °C (5.85 g, 90% yield). Elemental analysis, calc. for $C_{16}H_{27}NO_4Si$: C, 59.04; H, 8.36; N, 4.30; found: C, 58.72; H, 8.12; N, 4.10. IR (KBr) ν: 1634 cm^{-1} (C=N). ^1H NMR ($CHCl_3$) δ: 13.5 ppm (s, 1H, —OH), 8.32 ppm (s, 1H, —CH=N), 7.25 ppm (m, 2H, Ph), 6.96 ppm (d, 1H, Ph), 6.85 ppm (t, 1H, Ph), 3.85 ppm (q, 6H, —OCH_2), 3.60 ppm (t, 2H, —NCH_2), 1.85 ppm (q, 2H, CH_2), 1.22 ppm (t, 9H, CH_3), 0.68 ppm (t, 2H, —$SiCH_2$). UV/vis: λ_{max} (CH_2Cl_2) 325 nm.

2.2.2. Preparation of the zinc(II) complex ZnL_2

Zinc(II) acetate dihydrate (0.50 mmol, 0.11 g) and HL (1 mmol, 0.33 g) were mixed in 30 ml of ethanol and stirred at room temperature. The reaction mixture was checked by absorption UV/vis spectroscopy which, after a reaction time of 4 h, clearly showed that the imine band at 325 nm disappeared and a band at 361 nm appeared, concurrent with the formation of ZnL_2. This reaction product was not separated from the reaction mixture and in the subsequent reactions with the mesoporous silica hosts, ZnL_2 was reacted using 1 ml of the described reaction mixture. The workup of the reaction mixture, removing part of the solvent under reduced pressure, gave a solid yellow-green product, $(ZnL_2)^*$, in a 45% yield which account for the hydrolyzed ZnL_2 derivative containing two —$Si(OH)_3$ groups instead of the initial two —$Si(OEt)_3$ groups. Mp > 350 °C. Elemental analysis, calc. for $C_{20}H_{28}N_2O_8Si_2Zn$: C, 43.99; H, 5.17; N, 5.13; found: C, 44.54; H, 5.44; N, 5.02. IR (KBr) ν: 1619 cm^{-1} (C=N). As the complex was insoluble in common solvents, no ^1H NMR analysis was carried out.

The luminescence properties of Zn(II) imine complexes arise from the Zn(II) coordination sphere (see below) [33–35]. Therefore, the $(ZnL_2)^*$ photophysical data λ_{em} = 457 nm and Φ = 4.4%, as recorded on a powder sample, were used to compare the luminescence of materials synthesized using GPS and OPS.

2.2.3. Preparation of MCM-41

MCM-41 was prepared from a gel with the following molar composition: TEOS:NH_4OH:CTABr:H_2O = 1:1.64:0.15:126. In a typical synthesis, 2.40 g of CTABr were dissolved in 120 ml of ultrapure water and stirred until the washed solution was homogeneous and clear. After adding 8 ml of ammonium hydroxide (32 wt%), the mixture was stirred for 5 min, after which 10 g of TEOS was added. The solution was stirred overnight, filtered and washed with water and ethanol. For template removal and access to porosity, the solids are calcined at 823 K for 5 h.

2.2.4. Preparation of MCM-48

MCM-48 was prepared from gel with the following molar composition: TEOS:NaOH:CTABr:H_2O = 1:0.25:0.65:62. In a typical synthesis, 23 g of CTABr was dissolved in 111 ml of ultrapure water, then 1 g of sodium hydroxide and 20.80 g of TEOS were added. The solution was stirred for 1 h, transferred into a polypropylene bottle and heated at 383 K for 3 days. The solid was recovered by filtration, washed with distilled water, and calcined at 823 K for 6 h.

2.2.5. Preparation of SBA-15

Triblock copolymer was used as surfactant in the synthesis of SBA-15. The molar composition of the gel, for 4.0 g of Pluronic P123 was: TEOS:HCl:H_2O = 1:5.85:162.7. In a typical synthesis the block polymer was dissolved in 30 ml of water and 120 ml of chloride acid (2 M) solution and stirred constantly. Then 8.50 g of TEOS was added to the solution and stirring continued at 308 K for 20 h. The mixture was aged at 353 K overnight without stirring. The solid product was recovered, washed, and air-dried at room temperature. The template was removed by calcination at 773 K for 5 h.

Because in the following the properties of these starting materials will be compared with those of the grafted samples, MCM-41, MCM-48 and SBA-15 will be indicated, for clarity, as (GPS)(MCM-41), (GPS)(MCM-48) and (GPS)(SBA-15), respectively.

2.2.6. Preparation of (GPS)(HL/MCM-41), (GPS)(HL/MCM-48) and (GPS)(HL/SBA-15)

The procedure of grafting post-synthesis is the same for all the selected mesoporous silica solid products.

The incorporation of HL was performed on surfactant-free materials, by adding, under nitrogen atmosphere, an ethanolic solution containing the amount of HL (1 ml) required for a HL/SiO_2 molar ratio ≅ 3, to a suspension of 1 g of calcined mesoporous powder in 100 ml of ethanol. This mixture was refluxed under stirring for 17 h and the resulting solid was filtered, washed with ethanol and acetone, and dried in an oven at 333 K overnight. IR (KBr) ν: 1647 cm^{-1} (C=N for (GPS)(HL/MCM-41)); 1647 cm^{-1} (C=N for (GPS)(HL/MCM-48)); 1637 cm^{-1} (C=N for (GPS)(HL/SBA-15)). (HL/SiO_2: for (GPS)(HL/MCM-41) = 0.08; for (GPS)(HL/MCM-48) = 0.40; (GPS)(HL/SBA-15) = 0.43).

2.2.7. Preparation of (GPS)(Zn/MCM-41), (GPS)(Zn/MCM-48) and (GPS)(Zn/SBA-15)

The procedure of grafting post-synthesis is the same for all the selected mesoporous silica solids produced. The incorporation of Zn(II) chromophore was performed on the surfactant-free materials, by addition, under nitrogen atmosphere, of 1 ml of the above described ethanolic solution containing ZnL_2, to a suspension of 1 g of calcined mesoporous powder in 100 ml of ethanol (ZnL_2/SiO_2 molar ratio ≅ 3). This mixture was refluxed under stirring for 17 h. The resulting solid was filtered, washed with ethanol and acetone, and dried in oven at 333 K overnight. IR (KBr) ν: 1631 cm^{-1} (C=N for (GPS)(Zn/MCM-41)); 1634 cm^{-1} (C=N for (GPS)(Zn/MCM-48)); 1634 cm^{-1} (C=N for (GPS)(Zn/SBA-15)).

2.3. One-pot synthesis method

2.3.1. Preparation of (OPS)(Zn/MCM-41)

CTABr (2 g) was dissolved in 84 ml of distilled water. Then 23.88 ml of sodium hydroxide (1 M) was added to the solution and stirred for 10 min. Successively 9.40 g of TEOS and 1 ml of the above-described ethanolic solution containing ZnL_2 was added (ZnL_2/SiO_2 molar ratio ≅ 2). The mixture was stirred for 48 h at room temperature and the resulting solid was recovered by filtration, washed with ultrapure water, extracted twice with ethanol (1 g of solid for 500 ml of ethanol) and dried at 333 K overnight. IR (KBr) ν: 1634 cm^{-1} (C=N).

2.3.2. Preparation of (OPS)(Zn/MCM-48)

CTABr (2.40 g) was dissolved in a mixture of 100 ml of distilled water and 50 ml of EtOH. Then 12 ml of ammonium hydroxide (32 wt%), 3.40 g of TEOS and 1 ml of the ethanolic solution containing ZnL_2 (ZnL_2/SiO_2 molar ratio ≅ 2) were added. The mixture was stirred for 5 h at room temperature. After reaction, the solid was recovered by filtration, washed with distilled water, extracted two times with ethanol (1 g of solid for 500 ml of ethanol) and dried at 333 K overnight. IR (KBr) ν: 1634 cm^{-1} (C=N).

2.3.3. Preparation of (OPS)(Zn/SBA-15)

Pluronic P123 (4.0 g) was dissolved and stirred in 30 ml of water and 120 ml of chloridric acid (2 M). Then 8.50 g of TEOS and 1 ml of the above-described ethanolic solution containing ZnL_2 were added (molar ZnL_2/SiO_2 molar ratio ≅ 2) to the mixture and stirred for 20 h. The solid product was recovered, washed with distilled water, extracted twice with ethanol (1 g of solid for 500 ml of ethanol) and air-dried at 333 K overnight. IR (KBr) ν: 1634 cm^{-1} (C=N).

2.3.4. Preparation of (OPS)(MCM-41), (OPS)(MCM-48) and (OPS)(SBA-15)

In order to compare the properties of materials before and after functionalization, three reference samples were prepared using the same synthesis procedure of one-pot method, without adding ZnL_2.

2.4. Characterization

Elemental analysis was performed using a PerkinElmer CHNS/O 2400 apparatus and thermogravimetric data (TGA) were obtained with a Netzsch 409 analyzer. The infrared spectra were recorded on a KBr pellet using a PerkinElmer Spectrum One FT-IR spectrophotometer equipped for reflectance measurements. ^{1}H NMR spectra were recorded on a Bruker WM spectrometer at 300 MHz. Compounds were dissolved in deuterated chloroform ($CDCl_3$), and tetramethylsilane (TMS) was used as internal standard. X-ray diffraction (XRD) patterns of the powder samples were obtained with Cu Kα radiation on a Philips PW 1730/10 instrument. Measurements were performed in a 2θ range of 1–15° range with a step size of 0.005° and a step time of 0.5 s. Nitrogen adsorption–desorption measurements was measured at 77 K on a Micromeritics ASAP 2010. After template removal, the samples were pre-treated under vacuum at 623 K, or at 387 K for the functionalized samples, for 6 h before analysis. The specific surface area of samples was calculated using the BET model. Pore size distribution curves were obtained with the BJH (Barrett–Joyner–Halenda) method based on the desorption branch of the isotherms. It was impossible to record the absorption spectrum of the samples because the powder is too opaque for the transmission spectroscopy. It was tried to record an absorption spectrum using the reflectance spectroscopy, but the signal was too weak, due to the intense scattering. Corrected luminescence spectra were obtained on a Horiba Jobin Yvon Fluorolog 3 spectrofluorimeter, equipped with a Hamamatsu R-928 photomultiplier tube. The emission quantum yields of powder samples were obtained by means of a 102 mm diameter integrating sphere coated with Spectralon® and mounted in the optical path of the spectrofluorimeter using, as excitation source, a 450 W Xenon lamp coupled with a double-grating monochromator for selecting wavelengths. The experimental uncertainties were 1 nm for the band maxima for the luminescence spectra and 5% for EQY.

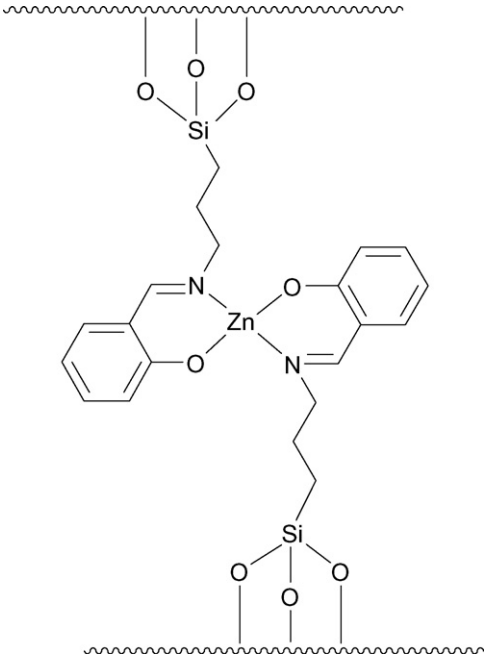

Fig. 1. Sketch of a possible chemical structure of the mesoporous-matrix-linked ZnL_2 complex.

3. Results and discussion

Chemically functionalized mesoporous materials incorporating ZnL_2 as a guest molecule were successfully obtained from both the method of GPS as well as the one-pot synthesis (OPS) procedure (Fig. 1).

3.1. Grafting post-synthesis products: (GPS)(Zn/MCM-41), (GPS)(Zn/MCM-48) and (GPs)(Zn/SBA-15)

The GPS method consists of two subsequent steps (Section 2). In the first, once surfactant has been removed by calcination, the host silica-based mesoporous material formed by silica-surfactant self-assembling [12] occurs simultaneously with the condensation of the inorganic species (TEOS). The second step is the post-synthesis incorporation of the ZnL_2 guest molecule onto the selected mesoporous supports, MCM-41, MCM-48 or SBA-15.

Successful grafting of the ZnL_2 was evidenced by the infrared (IR) spectra of the (GPS)(Zn/MCM-41), (GPS)(Zn/MCM-48) and (GPS)(Zn/SBA-15) products which show the absorption bands characteristic of the C=N stretching at 1631 cm^{-1} for (GPS)(Zn/MCM-41) or at 1634 cm^{-1} for both (GPS)(Zn/MCM-48) and (GPS)(Zn/SBA-15). These bands are shifted by ca. 10 cm^{-1} to lower values with reference to the corresponding (GPS)(HL/MCM-41), (GPS)(HL/MCM-48) and (GPS)(HL/SBA-15) reference compounds, thus reproducing the trend usually observed with metal complexation to an imino ligand [36].

The amount of the ZnL_2 loading can be conveniently represented by the ZnL_2/SiO_2 molar ratio. These values are obtained from the experimental TGA data (Table 1) of GPS samples and similar ZnL_2/SiO_2 ratios ranging from 0.09 for (GPS)(Zn/MCM-41) to 0.13 for (GPS)(Zn/SBA-15) were found. Since the reacted ZnL_2 was in large excess with respect to SiO_2 ($ZnL_2/SiO_2 \cong 3$), these results show that ZnL_2 can be successfully grafted on all three host materials used regardless of their different structures.

The pore structure and channel arrangement of the synthesized materials were studied with XRD powder diffraction (Figs. S1–S3 in SI), comparing the peaks pattern of the host (GPS)(MCM-41), (GPS)(MCM-48) or (GPS)(SBA-15) starting materials with those of the corresponding (GPS)(Zn/MCM-41), (GPS)(Zn/MCM-48) and (GPS)(Zn/SBA-15) derivatives (Table 2). The (GPS)(MCM-41) and (GPS)(MCM-48) materials did not exhibit high angle diffraction peaks, but only a broad band alongside the main reflection peak (*100*). The absence of high angle peaks is typical of poorly ordered long range porous systems. The XRD pattern of (GPS)(SBA-15) showed peaks corresponding to the (*100*), (*110*) and (*200*) reflections which are diagnostic of the *p6mm* hexagonal symmetry. After chemical modification, the (*100*) reflection was still detectable for all of the (GPS)(Zn/MCM-41), (GPS)(Zn/MCM-48) and (GPS)(Zn/SBA-15) series and approximately in the same position of the corresponding parent species (Table 2), suggesting that the pore arrangement of the grafted materials do not undergo significant modification.

Surface areas and pore volumes were analyzed using the nitrogen adsorption/desorption technique (Table 3). The N_2 adsorption isotherms of (GPS)(Zn/MCM-41) and (GPS)(Zn/MCM-48) exhibit typical Type IV reversible isotherms while (GPS)(Zn/SBA-15) showed Type IV irreversible isotherms with a hysteresis loop (Figs. S7–S9 in SI). The shift in nitrogen uptake, together with a decrease in pore volume, suggests that ZnL_2 occupies only part of the available space in the materials.

The physical properties of the investigated samples, compared in Table 3, demonstrate that ZnL_2 incorporation influences the adsorption properties, and show that ZnL_2 incorporation is governed by the topology of the starting material. In fact, the specific surface area of the Zn complex-containing materials is reduced as a function of the pore dimensions of the starting material: the greatest degree of reduction (32%) was found with (GPS)(Zn/SBA-15) ($D_{pore} \approx 50$ Å), a 30% reduction for

Table 1
ZnL_2/SiO_2 ratio obtained through thermogravimetric analysis.

Sample	Ratio ZnL_2/SiO_2	
	(GPS)	(OPS)
(Zn/MCM-41)	0.09	0.14
(Zn/MCM-48)	0.12	0.42
(Zn/SBA-15)	0.13	0.45

Table 2
XRD *d*-spacing of the synthesized siliceous mesoporous samples.

Sample	(GPS)			(OPS)		
	d_{100}	d_{110}	d_{200}	d_{100}	d_{110}	d_{200}
(MCM-41)	4.2			3.9		
(Zn/MCM-41)	4.5			4.2		
(MCM-48)	3.3			3.4		
(Zn/MCM-48)	3.4			3.8		
(SBA-15)	9.2	5.5	5.6	9.1	5.5	5.5
(Zn/SBA-15)	9.5	4.7	5.3	9.7	5.2	5.7

Table 3
Specific surface area calculated with the BET model (S_{BET}), nitrogen adsorption/desorption data (V_p), pore diameter (D_{pore}) of mesoporous materials.

Sample	S_{BET} (m^2/g)		V_p at (cm^3/g) $P/P_0 = 0.8$		D_{pore} (Å)	
	(GPS)	(OPS)	(GPS)	(OPS)	(GPS)	(OPS)
(MCM-41)	1135	1057	0.68	0.68	30	29
(Zn/MCM-41)	963	898	0.60	0.61	28	27
(MCM-48)	1357	1238	0.79	0.72	33	28
(Zn/MCM-48)	953	912	0.66	0.52	26	26
(SBA-15)	860	822	0.89	0.80	47	41
(Zn/SBA-15)	578	538	0.61	0.66	40	37

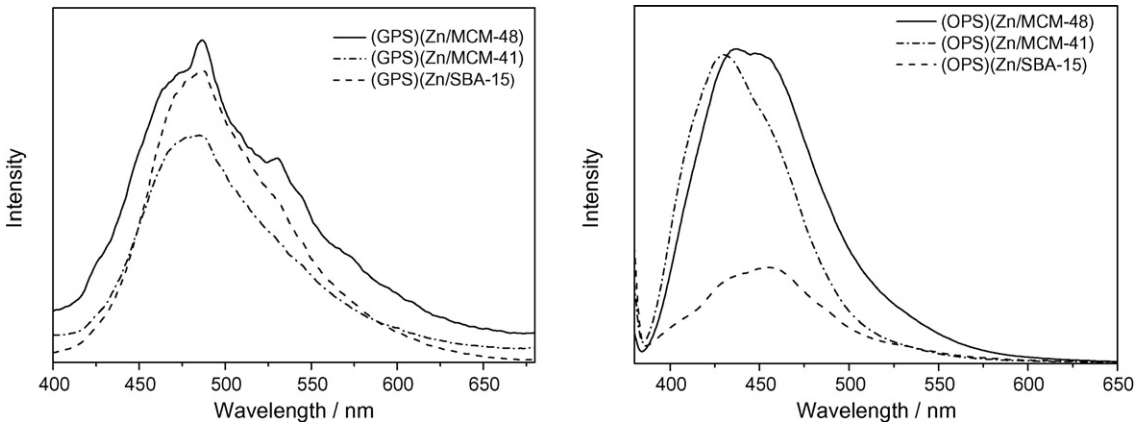

Fig. 2. Fluorescence emission spectra of mesoporous hybrid samples.

(GPS)(Zn/MCM-48) ($D_{pore} \approx 35$ Å), and only 15% for (GPS)(Zn/MCM-41) ($D_{pore} \approx 30$ Å). Considering the limited ZnL_2 loading (TGA) in the grafted materials, the reduction of surface area and pore volume, it can be supposed that grafting post-synthesis loading allows for a distribution of the guest species probably most on the external surface of the mesoporous hosts or near the channel openings. The luminescent properties of functionalized samples by grafting were investigated using emission spectra of powder samples sandwiched between two quartz windows (Fig. 2). Mesoporous materials without zinc(II) complex do not show luminescence, while the samples hosting the Zn(II) species (GPS)(Zn/MCM-41), (GPS)(Zn/MCM-48) and (GPS)(Zn/SBA-15) exhibited an emission maximum at 485 nm and an intense shoulder at about 530 nm.

The EQY of the GPS samples are independent of the type of mesoporous support, showing similar values, i.e. about 2% (Table 4). ZnL_2 emission is peaked at 457 nm, while the spectral bands of the GPS samples are red-shifted. The bands shape and the comparison with similar compounds [13,33] indicate that luminescence originates from singlet π–π^* ligand-centered excited state, which is lowered in energy respect to the non-emissive n–π^* iminic state as a consequence of the metal complexation. The spectral red-shift and the decreasing of the EQY of the GPS samples respect to reference compound (2% vs. 4.4%, respectively) could be due to a distortion of the geometry around the metal centre, which implies a mixing between and n–π^* and π–π^* related states; owing to this, the EQY reduces and the Franck-Condon shift enlarges. Moreover, the presence of two principal bands (at 485 and 530 nm) with different red-shift probably accounts for two principal types of confinement, whereby ZnL_2 is grafted on both the external surface and near the opening of the channels. Because these types of immobilization are independent of the type of mesoporous supports used, the EQY is expected to remain almost constant.

3.2. One-pot synthesis products: (OPS)(Zn/MCM-41), (OPS)(Zn/MCM-48) and (OPS)(Zn/SBA-15)

The syntheses of the materials functionalized using the one-pot method, (OPS)(Zn/MCM-41), (OPS)(Zn/MCM-48) and (OPS)(Zn/SBA-15), were carried out in a single step (Section 2) by reacting ZnL_2 and TEOS, in a molar ratio for $ZnL_2/SiO_2 \cong 2$. The incorporation of ZnL_2 was confirmed by IR spectroscopy, which showed the C=N stretching at values 1648 cm^{-1} for (OPS)(Zn/MCM-41) and 1634 cm^{-1} for both (OPS)(Zn/MCM-48) and (GPS)(Zn/SBA-15), comparable with those recorded for the corresponding compounds of the GPS series (Section 2). Quantitatively, the amount of loaded ZnL_2, given by the ZnL_2/SiO_2 ratios calculated from the TGA data (Table 1) is 0.14 for (OPS)(Zn/MCM-41), 0.43 for (OPS)(Zn/MCM-48) and 0.45 for (OPS) (Zn/SBA-15). Interestingly, these values, compared with those obtained for the GPS series, confirm that the ZnL_2 loading obtained from the one-pot method is more efficient that that obtained from grafting post-synthesis.

TGA data (Table 1) also show differences among these mesoporous "hosts" as a function of their structure and pore dimensions. The sample with higher amount of ZnL_2 is (OPS)(Zn/SBA-15) due to its larger pore size; samples of (OPS)(Zn/MCM-48) also contained a high amount of ZnL_2 due to the interconnected and three-dimensional channel network of the base material. In fact, such 3-dimensional channel is more efficient in loading than the one- and bi-dimensional channel of MCM-41 and SBA-15 materials, respectively.

X-Ray diffraction, N_2 adsorption/desorption and emission spectroscopy were used to investigate the topology of functionalized mesoporous materials. As seen with the GPS method, XRD patterns showed that functionalization did not alter the texture of the solids, as the hybrid samples exhibited the same structures as the reference samples MCM-41, MCM-48 and SBA-15 materials. The incorporation of the chromophore molecules into the framework was confirmed by an increase in intensity of XRD patterns (Figs. S4–S6 in SI). Samples (OPS)(Zn/MCM-41), (OPS)(Zn/MCM-48) and (OPS)(Zn/SBA-15) exhibited adsorption/desorption isotherms (Figs. S10–S12 in SI) similar to the grafted samples. In the OPS samples, however, the decrease in surface area and pore volume was greater in the ZnL_2-free reference samples than the GPS products. This result is in agreement with the TGA data, corresponding to a higher ZnL_2 content (Table 1).

The emission spectra for OPS samples (Fig. 2) showed an intense peak at 455 nm, and, contrary to spectra from the GPS samples, no relevant shoulders at higher wavelengths were detected. Furthermore, in this case, the EQY was dependent on the mesoporous topology, increasing as pore diameters decreased: (OPS)(Zn/MCM-41) with smaller pores exhibited highest EQY value (22%), while (OPS)(Zn/SBA-15) with large channels showed the lowest EQY (5%). The blue-shift of the emission maximum, related to a greater Frank-Condon shift respect to GPS samples, and the close resemblance with the free ZnL_2, reflect the minor distortion of the chromophore

Table 4
Emission quantum yield (EQY) of the Zn(II) complex-containing mesoporous materials.

Sample	Φ	
	(GPS)	(OPS)
(Zn/MCM-41)	2%	22%
(Zn/MCM-48)	2%	10%
(Zn/SBA-15)	2%	5%

in samples obtained via OPS with respect to GPS. Considering the trend of EQY, the intense emission of the OPS mesoporous materials could be attributed to the confinement of the chromophores in the walls of the silica matrix and within the channels since in this way, pore size reduction could confers to the luminophore an increased rigidity and a more efficient radiative deactivation. Similar conclusions have been reported for analogous systems in which conformational restriction of the rigid conjugate system gives rise to fluorescence enhancement [37,38].

4. Conclusions

The covalent incorporation of a luminescent $Si(OEt)_3$-functionalized Schiff base ZnL_2 in silica-based mesoporous materials has been successfully accomplished with two different synthetic procedures: grafting post-synthesis and one-pot synthesis. The structural properties and luminescent behavior of these host–guest complexation systems were studied using XRD, N_2 adsorption/desorption, TGA and UV/vis spectroscopy. In particular, for the first time the luminescent behavior of a LHMS solid samples was quantitatively investigated by direct measurement of the EQY utilizing an integrating sphere coupled with a spectrofluorimeter; in this way, it was possible to evidence a correlation between luminescence intensity and structure of mesoporous materials.

In summary, the photophysical characterization coupled with the usual investigation of the samples casts light on the chromophore distribution in doped mesoporous materials. The ZnL_2 amount and the EQY in GPS samples is constant, regardless of the type of starting mesoporous material, suggesting that ZnL_2 is principally anchored on the external walls and near the opening of the channels. Besides, reduction of the S_{BET} after grafting (which was proportional to the pore diameter) indicates that the channel openings are involved in the grafting of the chromophore. In OPS samples, the blue-shift of the emission band respect to GPS samples, the increase in EQY and the decrease in ZnL_2 loading which reflects the reduced pore diameter of the starting material, could be referred to an anchorage of ZnL_2 principally into the walls and within the channels.

With respect to grafting, the one-pot method is simpler in terms of synthesis protocols, offering a better control of organosilane ZnL_2 complex loading, and consequently a highly homogeneous distribution of organic groups. The best luminescent properties were obtained in materials synthesized from the one-pot synthesis. Since a tight chromophore confinement can significantly increase the EQY, the present data suggest that MCM-41, which presents a honeycomb-like structure of uniform mesopores is the most suitable host, providing the best fit for the Zn chromophores used here.

These results clearly indicate that one-pot synthesis is a reliable procedure for preparing high performing luminescent materials. It should also be mentioned that utilization of ZnL_2-loaded MCM-41 is of advantage to the fabrication of organic light emitting devices (OLEDs). Since the pathways open for n/p migration-recombination are limited essentially to only one dimension, it may be possible to obtain a grater degree of order on electroluminescent processes by utilizing porous, channel-type materials containing light-emitting and electronically interacting guest molecules [37,38].

Supporting information available

XRD patterns and adsorption/desorption isotherms for synthesized materials.

Acknowledgments

This research was supported by the Italian Ministero dell'Università e della Ricerca (MiUR) through the Centro di Eccellenza CEMIF.CAL (CLAB01TYEF) grant.

Appendix A. Supplementary data

Supplementary data associated with this article can be found, in the online version, at doi:10.1016/j.jphotochem.2008.10.001.

References

[1] F. Hoffmann, M. Cornelius, J. Morell, M. Fröba, Angew. Chem. Int. Ed. 45 (2006) 3216.
[2] G.J.A.A. Soler-Illia, P. Innocenzi, Chem. Eur. J. 12 (2006) 4478.
[3] S. Angelos, E. Johansson, J.F. Stoddart, J.I. Zink, Adv. Funct. Mater. 17 (2007) 2261.
[4] B.J. Scott, G. Wirnsberger, G.D. Stucky, Chem. Mater. 13 (2001) 3140.
[5] H. Parala, H. Winkler, M. Kolbe, A. Wohlfart, R.A. Fischer, R. Schmechel, H. von Seggern, Adv. Mater. 12 (2000) 1050.
[6] Y.J. Han, J.M. Kim, G.D. Stucky, Chem. Mater. 12 (2000) 2068.
[7] D. Chandra, T. Yokoi, T. Tatsumi, A. Bhaumik, Chem. Mater. 19 (2007) 5347.
[8] C.J. Brinker, G.W. Scherer, Sol–Gel Science, Academic Press, New York, 1990.
[9] C.J. Brinker, D.E. Clark, D.R. Ulrich (Eds.), Better Ceramics through Chemistry, North-Holland, New York, 1984, pp. 1–847.
[10] J.D. Mackenzie, D.R. Ulrich (Eds.), Ultrastructure Processing of Advanced Ceramics, Wiley, New York, 1988, pp. 1–564.
[11] R.K. Iler, The Chemistry of Silica, Wiley-Interscience, New York, 1979, pp. 1–866.
[12] R. Reisfeld, C.K. Jørgensen, Chemistry, Spectroscopy and Applications of Sol–Gel Glasses, Structure and Bonding, vol. 77, Springer, Berlin, 1992.
[13] H. Zhang, P. Zhang, K. Ye, Y. Sun, S. Jian, J. Wang, W. Pang, J. Lumin. 117 (2006) 68.
[14] Y. Lu, H. Fan, N. Doke, D.A. Loy, R.A. Assink, D. Lavan, C.J. Brinker, J. Am. Chem. Soc. 112 (2000) 5258.
[15] T. Asefa, M.J. MacLachlan, N. Coombs, G.A. Ozin, Nature (1999) 867.
[16] E. DeOliveira, C.R. Neri, O.A. Serra, A.G.S. Prado, Chem. Mater. 19 (2007) 5437.
[17] L.-N. Sun, J.-B. Yu, H.-J. Zhang, Q.-G. Meng, E. Ma, C.-Y. Peng, K.-Y. Yang, Microporous Mesoporous Mater. 98 (2007) 156.
[18] S. Bo, X. Liu, Z. Zhen, Preparation and luminescence properties of hybrid materials containing lanthanide complexes covalently bonded to a terpyridine-functionalized silica matrix, J. Lumin. 128 (2008) 1725.
[19] L.-N. Sun, Y. Zhang, J.-B. Yu, C.-Y. Peng, H.-J. Zhang, Ternary lanthanide (Er^{3+}, Nd^{3+}, Yb^{3+}, Sm^{3+}, Pr^{3+}) complex-functionalized mesoporous SBA-15 materials that emit in the Near-Infrared range, J. Photochem. Photobiol. A: Chem. 199 (2008) 57.
[20] S. Quici, M. Cavazzini, M.C. Raffo, L. Armelao, G. Bottaro, G. Accorsi, C. Sabatini, F. Barigelletti, J. Mater. Chem. 16 (2006) 741.
[21] L.C. Cides da Silva, T.S. Martins, M. Santos Filho, E.E.S. Teotonio, P.C. Isolani, H.F. Brito, M.H. Tabacniks, M.C.A. Fantini, J.R. Matos, Microporous Mesoporous Mater. 92 (2006) 94.
[22] A. Fernandes, J. Dexpert-Ghys, A. Gleizes, A. Galarneau, D. Brunel, Microporous Mesoporous Mater. 83 (2005) 35.
[23] Q.G. Meng, P. Boutinaud, A.C. Franville, H.J. Zhang, R. Mahiou, Microporous Mesoporous Mater. 65 (2003) 127.
[24] P. Escribano, B. Julian-Lopez, J. Planelles-Aragò, E. Cordoncillo, B. Vianab, C. Sanchez, J. Mater. Chem. 18 (2008) 23.
[25] M. Ogawa, T. Nakamura, J.-I. Mori, K. Kuroda, Microporous Mesoporous Mater. 48 (2001) 159.
[26] B. Lei, B. Li, H. Zhang, W. Li, J. Phys. Chem. C 111 (2007) 11291.
[27] A.B. Descalzo, M. Dolores Marcos, C. Monte, E. Martinez-Manez, K. Rurack, J. Mater. Chem. 17 (2007) 4716.
[28] S.-J. Seo, D. Zhao, K. Suh, J.H. Shin, B.-S. Bae, J. Lumin. 128 (2008) 565.
[29] M.H.V. Werts, R.T.F. Jukes, J.W. Verhoeven, Phys. Chem. Chem. Phys. 4 (2002) 1542.
[30] A. Crispini, I. Aiello, M. La Deda, I. De Franco, M. Amati, F. Lelj, M. Ghedini, Dalton Trans. 43 (2006) 5124.
[31] K. Moller, T. Bein, Chem. Mater. 10 (1998) 2950.
[32] G.A. Ozin, E. Chomski, D. Khushalani, M.J. MacLachlan, Curr. Opin. Colliod Interface Sci. 3 (1998) 181.
[33] M. La Deda, M. Ghedini, I. Aiello, A. Grisolia, Chem. Lett. 3 (2004) 1060.
[34] T. Sano, Y. Misho, Y. Hamada, H. Takahashi, T. Vsuky, K. Ghibata, J. Mater. Chem. 10 (2000) 157.
[35] P. Wang, Z. Hang, Z. Xie, S. Tang, O. Wong, C.-S. Lee, N. Wong, L. Hung, S. Lee, Chem. Commun. (2003) 1664.
[36] T. Yu, W. Su, W. Li, Z. Hong, R. Hua, M. Li, B. Chu, B. Li, Z. Zhang, Z.Z. Hu, Inorg. Chim. Acta 359 (2006) 2246.
[37] L.Z. Zhang, Y. Xiong, P. Cheng, G.-Q. Tang, D.-Z. Liao, Chem. Phys. Lett. 358 (2002) 278.
[38] L. Gao, Y. Wang, J. Wang, L. Huang, L. Shi, X. Fan, Z. Zou, T. Yu, M. Zhu, Z. Li, Inorg. Chem. 45 (2006) 6844.